

A MIMO-MLSE Receiver for Electronic Dispersion Compensation of Multimode Optical Fibers

Diego E. Crivelli* Hugo S. Carrer* Mario R. Hueda* Oscar E. Agazzi
Clariphy Communications, Inc.

16 Technology Drive, Suite 165 Irvine, CA, 92618, U.S.A.

Email: {diego.crivelli, hugo.carrer, mario.hueda, oscar.agazzi}@clariphy.com

*Digital Communications Research Laboratory, National University of Córdoba
Av. Vélez Sarsfield 1611, Córdoba (X5016GCA), Argentina

Email: {dcrivelli, hscarrer, mhueda}@com.uncor.edu

Abstract—In this paper we propose a multiple-input, multiple-output (MIMO) maximum-likelihood sequence estimation (MLSE) receiver for electronic dispersion compensation (EDC) of multimode optical fibers at 10Gb/s data rate. As the primary example of the effectiveness of the techniques introduced here we present a receiver for the emergent 10GBASE-LRM standard for 10Gb/s Ethernet over multimode optical fibers [1]. We show that an MLSE receiver provides an advantage of at least 2dB over other receivers, such as the decision-feedback equalizer (DFE), on 99% of the local area network (LAN) multimode fiber population, as modeled by a database proposed by the IEEE 802.3aq Task Force [2]. The paper deals with both theoretical and practical aspects of the architecture. To enable the complete integration of this receiver as a single chip in current 90nm CMOS technology, we propose the parallel-processing digital implementation of a feedforward equalizer (FFE) and a Viterbi decoder together with an interleaved front-end analog to digital converter (ADC). The MIMO structure jointly compensates for fundamental channel impairments such as multimode dispersion, and implementation-related effects such as the limitations of the analog front end (AFE), particularly the one known as *fixed-pattern noise* (FPN) [3]. As a result of the high speed operation, FPN has a major impact on performance. We show that, without compensation, FPN could result in a degradation of 7.86dB. With the compensation proposed here, the latter is reduced to 0.23dB.

I. INTRODUCTION

Maximum-likelihood sequence estimation (MLSE) has attracted considerable interest in recent literature as an electronic dispersion compensation (EDC) technique for single-mode optical fibers, particularly for long-haul or metropolitan area network applications [4], [5], [6]. However, most of the literature on EDC for multimode fibers (MMF) is based on the decision-feedback equalizer [7], [8]. Multimode fibers are typically used in local area network (LAN) applications, in links whose length could reach or exceed 300 meters. A large percentage of the existing fiber population consists of legacy fibers that exhibit large multimode dispersion. Interest in EDC for MMF has grown significantly in recent years as a result of the standardization activities of the IEEE 802.3aq Task Force, which is developing the 10GBASE-LRM standard [1] for 10 Gb/s Ethernet over MMF based on the application of EDC technology. The MMF channel differs significantly from the single-mode channel, therefore the application of MLSE to MMF requires new investigations. Although some of the recent

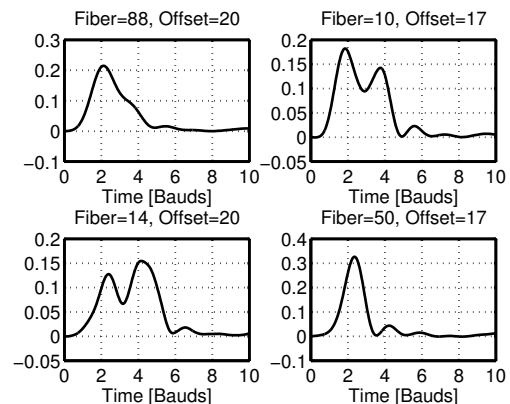


Fig. 1. Typical MMF impulse responses

literature [9], [10] mentions this topic, detailed architectural studies taking into account implementation constraints have not been reported so far. Figure 1 shows some typical MMF impulse responses [11]. In general, both the time span of the impulse responses and the variability of their shapes make equalization of MMF more difficult than that of single-mode fibers. For example, some recently proposed MLSE receivers for single-mode fibers do not include a feedforward equalizer (FFE). This may be motivated by the difficulty of implementing the FFE at 10 Gb/s data rate. However, we show in Section V that an MLSE receiver for MMF without an FFE would suffer an unacceptable performance loss of 3.5dB. It is interesting to mention that the response of some fibers may be nonstationary (this is also true for polarization mode dispersion (PMD) in single-mode fibers). Other impairments of the MMF channel include *relative intensity noise* (RIN), *modal noise* (MN), and *thermal noise*. These will be discussed in the next section. In addition to the intrinsic channel impairments, the optical receiver may have to cope with implementation-related impairments. In this paper, we investigate a digital signal processing (DSP) implementation for the MLSE receiver, where the only analog blocks are those that provide an interface with the external world. The most important of them is the input analog to digital converter (ADC). As will be seen in Section IV, we propose an interleaved architecture for the ADC [12] to meet the high sampling rate requirements with

current technology. However, the performance of interleaved ADCs is affected by gain and sampling phase errors, as well as offsets, that are not perfectly matched across the interleaved array [3]. A related effect occurs as a result of the mismatches of the frequency responses of the track and hold (T&H) amplifiers that typically precede the ADCs in the array. These effects are collectively referred to as *fixed-pattern noise*. In this paper, we are interested in both the fundamental properties of the channel that affect the receiver performance, such as multimode dispersion and optical noise components, and in the implementation-related impairments such as fixed-pattern noise. To jointly compensate for all of them, we propose a Multiple-Input, Multiple-Output (MIMO) MLSE receiver. We investigate the performance of the proposed receiver using computer simulations. In our simulations we use two different databases of optical fiber responses proposed by the IEEE 802.3aq Task Force, the *Cambridge Database* [11], and the *Monte Carlo Database* [2]. These databases are representative of the MMF population used in LAN applications, and they allow researchers and developers to make predictions about the percentage of fibers in the entire population over which a particular receiver architecture would be able to operate with a specified performance, for example bit error rate (BER) lower than 10^{-12} . Considering only the optical channel impairments, we show that the receiver proposed in this paper achieves at least a 2dB advantage over previously proposed receivers on 99% of the fibers in the Monte Carlo database. If we also consider implementation effects, the advantage of the receiver proposed here increases to at least 4dB. The rest of this paper is organized as follows. In Section II we present a MIMO formulation of the MMF channel, including the receiver AFE. In Section III we present the proposed MIMO-MLSE receiver. In Section IV we describe other aspects of the receiver architecture including some implementation considerations. In Section V we present simulation results. Finally, in Section VI we draw conclusions.

II. THE MULTIMODE FIBER CHANNEL - A MIMO FORMULATION

Throughout this paper, we use the channel proposed by the 10GBASE-LRM draft standard [1] as the primary example of application of the proposed techniques. However, while the fiber length specified by the draft standard is 220 meters, we assume a 300 meter length in our simulations (Section V). This is motivated by the large number of fibers in the field whose length approaches 300 meters, and by the fact that users of EDC technology have expressed a desire for this extended reach. Although with the goal of making our discussion more specific we have chosen the LRM channel as our primary example, the techniques proposed in this paper are general, and they can be used in many other fiber optic or electrical communications applications. Figure 2 shows a simplified diagram of the channel. The transmitter uses a 1310nm Fabry-Perot or DFB laser. Light can be launched into the MMF using either center or offset launch conditions [13]. At the receive end, the optical signal is detected by a PIN photodiode and

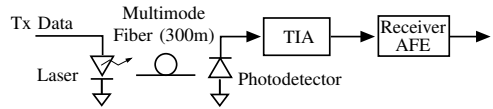


Fig. 2. Typical MMF channel

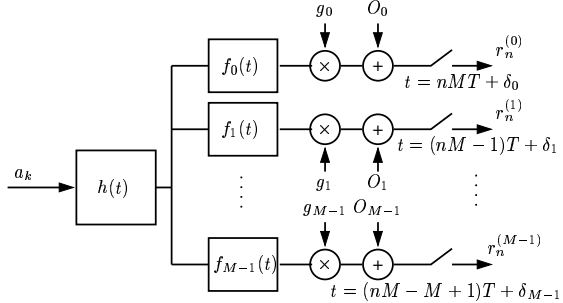


Fig. 3. MIMO channel model

the photocurrent is converted to a voltage and amplified using a transimpedance amplifier (TIA) and a linear post amplifier. Legacy MMF suffer from significant modal dispersion. Figure 1 shows some typical fiber impulse responses, taken from the Cambridge database. On some MMF, particularly under center launch conditions, the response may vary over time as a result of vibrations or mechanical stress on the fiber [14], [15]. Noise in MMF links is dominated by RIN, MN, and thermal noise [16]. While RIN and MN are nongaussian, thermal noise, mainly produced by the TIA at the input of the receiver, is Gaussian. In this work we assume that the noise is Gaussian. This is a reasonable approximation, since thermal noise is typically dominant in the LRM channel. Nonlinearity may be introduced in the signal by the laser and/or the TIA and post amplifier. For simplicity we neglect nonlinearity in our performance analysis.

In addition to the intrinsic channel impairments, the receiver has to cope with implementation-dependent impairments. In this paper, we treat these impairments as part of the channel.

Figure 3 shows a model of the communication link where the impairments of the analog front end, particularly the M -parallel time interleaved ADC system, are explicitly shown as part of the channel. Here, $h(t)$ models the optical channel response as well as the receive filter and any other linear element present in the link and $a_k \in \{-1, +1\}$ are the transmitted symbols. Blocks $f_0(t)$ to $f_{M-1}(t)$ model the independent frequency responses of each T&H unit. Gain errors and offsets are modeled by g_0 to g_{M-1} and O_0 to O_{M-1} , respectively. Finally, δ_0 to δ_{M-1} model sampling time errors. The output of the system is comprised by M parallel samples, $r_n^{(0)}$ to $r_n^{(M-1)}$, which will be processed by the MIMO receiver. Note that the superscript identifies baud spaced samples, whereas subscript n represents samples spaced M -baud periods apart. For simplicity, noise sources such as AWGN and quantization noise are not explicitly shown in the diagram.

First we transform filters $h(t)$ and $f_0(t)$ through $f_{M-1}(t)$ from the continuous to the sampled time domain. The transformation assumes ideal sampling (sampling without phase errors). Sampling time errors will be modeled with a MIMO

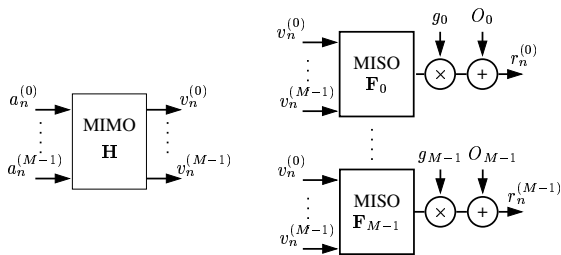


Fig. 4. Equivalent MIMO model of the channel.

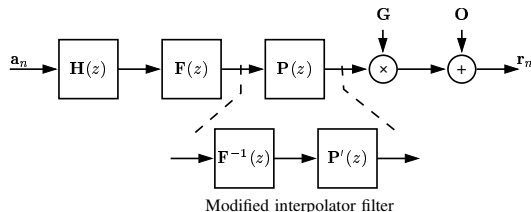


Fig. 5. MIMO model

interpolation filter, as will be seen later. Defining:

$$a_n^{(i)} = a_{(nM-i)} \quad i = 0, \dots, M-1, \quad (1)$$

a MIMO description of this communication link is obtained by converting the single-input, single-output (SISO) filters $h(t)$ and $f_0(t)$ through $f_{M-1}(t)$ to a MIMO and a multiple-input, single-output (MISO) representation, respectively (see Fig. 4). The MIMO and MISO models can be combined to obtain a single MIMO representation.

In this way, the MIMO model accepts M -dimensional input vectors whose components are transmitted symbols, and produces M -dimensional output vectors whose components are signal samples, at a rate $1/MT$. In Fig. 5 we show a detailed diagram of the MIMO model. The vector of input symbols \mathbf{a}_n feeds the channel response matrix $\mathbf{H}(z)$. The output of this channel is fed to the T&H matrix filter $\mathbf{F}(z)$, which models the independent T&H responses. $\mathbf{P}(z)$ models the sampling time errors. It can be seen as a block that interpolates the samples taken without sampling errors at the output of the channel and generates M outputs with sampling errors. With identical T&H responses, the sampling time errors can be modeled using an interpolation filter that generates samples with phase errors for each output of the MIMO model. When T&H responses are taken into account, a possible way to continue to use the interpolator filter is to invert the response of $\mathbf{F}(z)$, as is shown inside the dotted line of Fig. 5. While the use of an interpolation filter is completely accurate only when samples are free of aliasing, it can still be used as an approximation when there is some aliasing owing to T -spaced sampling and excess bandwidth greater than zero. This approximation is valid when sampling time errors are small, which is generally the case in the applications considered in this paper. Finally, matrix \mathbf{G} and vector \mathbf{O} represent gain and offsets errors, respectively. From Fig. 5, the MIMO model can be written as:

$$\mathbf{r}(z) = \mathbf{G}\mathbf{P}(z)\mathbf{F}(z)\mathbf{H}(z)\mathbf{a}(z) + \mathbf{O}(z). \quad (2)$$

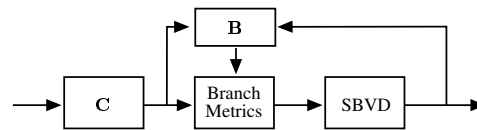


Fig. 6. MIMO-MLSE receiver.

Grouping the factors in the first term of the sum we obtain the entire MIMO response of the system in z -domain and time-domain, respectively:

$$\mathbf{r}(z) = \mathbf{S}(z)\mathbf{a}(z) + \mathbf{O}(z), \quad \mathbf{r}_n = \sum_{l=-\infty}^{\infty} \mathbf{S}_l \mathbf{a}_{n-l} + \mathbf{O}. \quad (3)$$

III. MIMO-MLSE EQUALIZATION

Given model (3), the joint compensation of the channel impairments (such as intersymbol interference (ISI)) and the AFE errors can be formulated as the general equalization problem of a MIMO channel [17]. Common equalization techniques include feed forward equalization, decision feedback equalization, and maximum likelihood sequence estimation. In this paper we analyze the MIMO-MLSE receiver (Fig. 6). This is motivated by the fact that the optimal receiver for an intersymbol interference channel in the presence of Gaussian noise consists of a whitened matched filter followed by a maximum likelihood sequence detector [18]. The receiver consists of a MIMO-FFE (\mathbf{C}) coupled to a sliding block Viterbi decoder (SBVD) and a MIMO channel estimator (\mathbf{B}). This architecture is able to compensate for the ISI of the MMF, as well as for the impairments of the receiver front-end, such as the independent T&H responses, gain errors, sampling phase errors and offset.

The MIMO-FFE is described by the following equation:

$$\mathbf{q}_n = \sum_{l=0}^{N_f-1} \mathbf{C}_l \mathbf{r}_{n-l} \quad (4)$$

where N_f is the number of $M \times M$ -matrix taps (\mathbf{C}_i) of the forward equalizer.

Let K be the total number of bits transmitted. It is convenient to assume, without loss of generality, that $K = NM$ with N integer. The maximum-likelihood sequence detector chooses, among the 2^K possible sequences, the one $\hat{\mathbf{A}}_n = (\hat{a}_{nM}, \hat{a}_{nM-1}, \dots, \hat{a}_{(n-1)M-\Delta+2})$ that minimizes the metric:

$$m = \sum_{n=1}^N \|\mathbf{q}_n - \mathbf{B}(\hat{\mathbf{A}}_n)\|^2, \quad (5)$$

where $\mathbf{B}(\cdot)$ is a function that models the response of the equalized channel with memory $\Delta - 1$. Note that each component of $\mathbf{B}(\cdot)$ depends only on Δ consecutive received bits. In our formulation we assume that in general the function $\mathbf{B}(\cdot)$ is nonlinear. The minimization of (5) can be efficiently implemented using the Viterbi algorithm [18]. The required number of states of the Viterbi decoder is $S = 2^{\Delta-1}$. The SBVD [19] is the most suitable form of the Viterbi algorithm for a MIMO receiver. The input to the SBVD is the FFE output vector \mathbf{q}_n , and the output is a block of M detected symbols $\hat{\mathbf{a}}_n$.

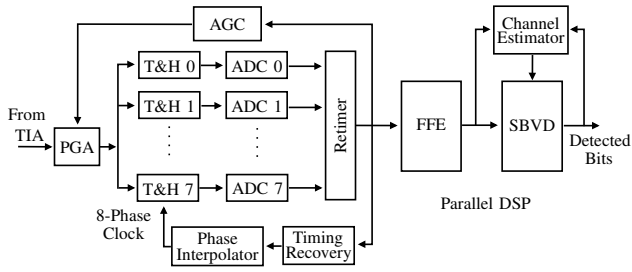


Fig. 7. Simplified block diagram of the receiver

The MIMO channel estimator generates the $2MS$ expected values $\mathbf{B}(\hat{\mathbf{A}}_n)$ of the M components of the \mathbf{q}_n vector for all possible combinations of the Δ most recent received bits (corresponding to the $2S$ branch metrics in the trellis diagram). The MIMO channel estimator can be implemented using M lookup tables, each lookup table having $2S$ entries.

The coefficients of the FFE and the lookup tables can be iteratively adapted using the well known LMS algorithm, as follows for iteration j :

$$\mathbf{e}_n = \mathbf{B}^j(\hat{\mathbf{A}}_n) - \mathbf{q}_n, \quad (6)$$

$$\mathbf{C}_l^{j+1} = \mathbf{C}_l^j + \beta \mathbf{e}_n \mathbf{r}_{n-l}^T, \quad (7)$$

$$\mathbf{B}^{j+1}(\hat{\mathbf{A}}_n) = \mathbf{B}^j(\hat{\mathbf{A}}_n) - \gamma \mathbf{e}_n \quad (8)$$

where $(\cdot)^T$ means transpose and β and γ are the algorithm step sizes of the FFE and channel estimator, respectively. The notation of (8) was slightly modified to include the iteration number j of the LMS update as a superscript.

IV. RECEIVER ARCHITECTURE

In this section we describe the proposed receiver architecture. We emphasize practical and implementation-related aspects. Figure 7 shows a simplified block diagram. The input signal comes from a photodetector and a TIA, which in this section will be treated as external. The level of the input signal is adjusted by a programmable gain amplifier (PGA), whose gain is controlled by a digital automatic gain control (AGC). The output of the PGA is applied to an array of eight interleaved T&H amplifiers followed by eight ADCs. The T&H amplifiers take samples of the input signal at a rate of 1289.0625Ms/s each, but the sampling clocks of the different interleaves are staggered in phase by 96.97ps, so that the signal is sampled at an aggregate rate of 10.3125Gs/s. This is also the symbol rate in the LRM channel, therefore the receiver samples the signal at the symbol rate. The phases of the eight sampling clocks are controlled by the digital timing recovery through an analog phase interpolator. In practice, small errors in the phases of these clocks exist as a result of slight mismatches in the delays of the clock distribution network, strength of clock buffers etc. These phase errors are one of the causes of the fixed pattern noise which in the formulation of Section II is a part of the channel model. Other sources of fixed pattern noise also included in the channel model are gain and offset mismatches in the T&Hs and ADCs, and frequency response mismatches of the T&H. The outputs of the eight ADCs are time-aligned and passed

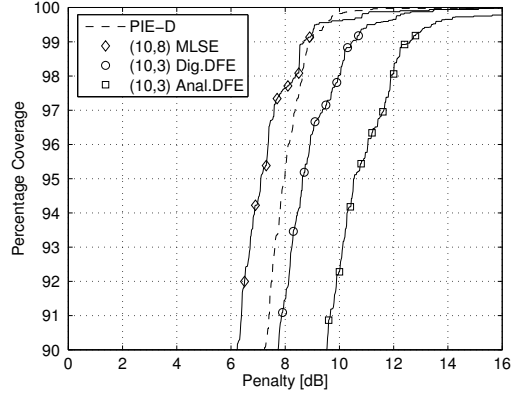


Fig. 8. Coverage of fiber population versus penalty for different receivers

to the parallel-processing DSP that implements the rest of the receiver. The most important DSP blocks are the AGC, the Timing Recovery, the MIMO-FFE, the sliding block Viterbi decoder, and the MIMO channel estimator. The number of taps of the FFE can be programmed by the user. This allows the user to trade performance for power consumption. For similar reasons, the number of states of the Viterbi decoder can be set by the user.

A. MIMO Model and Parallelism

The parallel implementation of the FFE [20] is closely related to the MIMO structure. From the MIMO representation, the FFE can be expanded as a convolution matrix as follows:

$$\mathbf{C} = \begin{bmatrix} c_0^{(0)} & c_1^{(0)} & \dots & c_{L_f-1}^{(0)} & 0 & \dots & 0 \\ 0 & c_0^{(1)} & c_1^{(1)} & \dots & c_{L_f-1}^{(1)} & \dots & 0 \\ 0 & 0 & \dots & \dots & \dots & \dots & 0 \\ 0 & 0 & \dots & c_0^{(M-1)} & c_1^{(M-1)} & \dots & c_{L_f-1}^{(M-1)} \end{bmatrix}, \quad (9)$$

where L_f is the number of taps used. Then the output samples are computed as:

$$\mathbf{q}_n = \mathbf{C} [r_{(nM)} \quad r_{(nM-1)} \quad \dots \quad r_{((n-1)M+L_f-1)}]^T \quad (10)$$

The parallel implementation of the FFE can be represented by M FIR filters, which is precisely what (10) represents. In the presence of mismatches in the AFE, the coefficients in different rows of (9) are different. On the other hand, if no mismatch errors exist, all rows of (9) become equal. This is the traditional parallel processing FIR structure [20]. In this particular case there is no need to adapt M independent sets of coefficients. The MIMO structure of the Viterbi decoder is also essentially identical to the parallel processing realization. The only modification is that branch metrics associated with different components of the input vector \mathbf{q}_n are computed using different components of the channel estimator function \mathbf{B} , which is not the case in a traditional parallel implementation. Although in equations (9) and (10) the implicit assumption is made that the DSP parallelization factor equals the dimension of the MIMO channel, in practice this constraint is not necessary.

V. SIMULATION RESULTS

In this section we present results of a simulation study of the receiver described in the previous sections. We use two different simulators. One of them, called OCCAM (Optical Communication Channel Analytic Model), is a very fast, Matlab [21] based tool that computes performance by solving the receiver equations. Because of its speed, this tool allows fundamental limits to be rapidly explored on large databases. The tool is particularly useful to compare different architectures, including limiting cases, for example finite or infinite decision feedback equalizers (DFE), finite or infinite MLSE receivers, etc. One particularly important ideal receiver is a DFE with infinite number of feedforward and feedback taps. This receiver is used in the 10GBASE-LRM draft standard to define an implementation-independent performance measure, called PIE-D (“*penalty of the ideal equalizer - DFE*”) [22]. The other simulator, called LiSST (Lightwave System Simulation Tool), is a C++ based fixed-point time domain simulator. It is asynchronous and event-driven, therefore it allows an arbitrary number of clock domains to be simulated. It accurately models nonstationary effects, such as timing recovery acquisition, jitter, etc. It is bit and clock cycle accurate, and it models the behavior of the DSP hardware with great accuracy. Extensive consistency checks of the two simulators have been carried out with excellent results.

The performance measure used for all receivers in this study is the probability of error P_e . However, for convenience of presentation, we also define the signal to noise ratio (SNR) which is related with P_e by $\sqrt{\text{SNR}} = Q^{-1}(P_e)$, where $Q(x) = 0.5\text{erfc}(x/\sqrt{2})$. A quantity more commonly used by the optical communications community is the *penalty*, which for the application of interest in this paper can be defined as $P = 30 - \text{SNR}_{\text{dB}}^1$. Penalty is a function of both the channel and the receiver. Higher penalties correspond to lower performance and higher error rates. For a more complete explanation of the concept of penalty, the reader is referred to [22]. For our purpose, it is sufficient to regard penalty as measure of performance, which is related to P_e . OCCAM computes P for each receiver using well known theory [17]. LiSST computes P_e using time domain simulations.

The performance of the proposed receiver and the DFE has been simulated on the Monte Carlo database. For clarity, we show only the (10,8) configuration of the MIMO-MLSE receiver, where the first number in the pair refers to the number of FFE taps, and the second is the number of states of the Viterbi decoder (recall from the previous section that these parameters are user programmable). For comparison, the performance of an infinite DFE (PIE-D) and a DFE with 10 T-spaced feedforward taps and 3 feedback taps is also presented (denoted DFE(10,3)). Recent literature [23] has described analog implementations of 10Gb/s equalizers where the delay line of the adaptive FIR filter is implemented using

second order sections as delay elements. The parameters of the second order section are optimized to achieve maximum bandwidth and an approximately linear phase characteristic. However, an intrinsic limitation of this architecture is that the delay elements have limited bandwidth and they degrade the equalizer performance. A DFE using these techniques has also been simulated for comparison with the other architectures. The power spectral density N_0 of noise at the input of the receiver in all the configurations simulated is set according to the methodology of [24]. The value of N_0 that results is such that a matched filter receiver operating in the absence of dispersion would have an SNR at the slicer of 30dB. Figure 8 shows the simulation results in the form of cumulative histograms of fiber coverage versus penalty. For a given value of abscissa, the ordinate of a point on the curve represents the percentage of fibers in the database for which the penalty of the corresponding receiver is less than or equal to the abscissa. The histograms show that the MIMO-MLSE receiver proposed here performs 2dB better than the digital DFE, and 4dB better than the analog DFE at 99% coverage. We have also simulated an 8-state MLSE receiver without an FFE. Such an architecture has been considered for single-mode fiber applications in recent literature. Although for clarity the corresponding curve is not shown in Fig. 8, the penalty at 99% coverage for this receiver is 3.5dB higher than for the MLSE(10,8) receiver. This shows that feedforward equalization is required in the LRM channel.

A. Compensation of Fixed Pattern Noise

The effectiveness of the MIMO architecture to compensate fixed-pattern noise was tested using LiSST. Simulations were run over 15 MMF channels selected randomly from the Cambridge database. Each channel in this database is uniquely identified by a fiber number and a launch offset (in microns). The channels we chose are identified by the following fiber/offset pairs: (57/17), (88/20), (84/17), (10/17), (108/20), (50/17), (19/20), (55/20), (57/20), (10/20), (60/23), (20/23), (70/23), (59/23), and (27/17).

Open loop T&Hs are among the most suitable for high speed applications [25, pp. 29]. The transfer function of the T&H is modeled as a two real pole system. One of the poles models the input buffer, whereas the other models the T&H circuit in track mode [26]. In our example, the poles are nominally located at -9 and -10GHz. With process variations of $\pm 20\%$, the poles fall in the range $K(-9, -10)$ GHz with $K = 0.8$ to 1.2. These variations across the constituent T&Hs in the interleaved array are responsible for one of the components of fixed-pattern noise. The values of mismatch used in the simulations for the other components of fixed-pattern noise were: $\pm 5\%$ for phase errors, $\pm 5\%$ for gain errors and $\pm 5\%$ for offset. The following cases are considered: 1) No mismatches; 2) Mismatch errors and MIMO equalizer; 3) Mismatch errors and SISO equalizer. SISO equalizer means a single set of coefficients for all the MIMO responses. We define the SNR loss of the MIMO scheme as the difference of SNR between cases 2 and 1 and the SNR loss for the SISO scheme as the

¹In the optical communications community it is common to measure penalties in *optical* dB, but throughout this paper we use *electrical* dB. Penalties expressed in optical dB are one half of those reported in this paper.

TABLE I
SUMMARY OF RESULTS OF SNR LOSS [dB]

Arch.	Offset	Gain	Samp.	BW	All, no offset	All
SISO	6.22	1.99	1.48	1.86	4.38	7.86
MIMO	0.01	0.04	0.04	0.11	0.20	0.23

equivalent difference between cases 3 and 1. In Table I we show the results. In order to simplify the presentation we have averaged them over the set of 15 fibers described before. The fact that the SNR loss of the MIMO equalizer is nonzero is a result of noise enhancement owing to the FFE equalization of the different channels. The table shows a degradation as high as 7.86dB for the SISO scheme. The degradation drops to 0.23dB for the MIMO scheme. From these results it can be seen that the architecture presented can effectively compensate for all mismatch impairments on the receiver front-end.

VI. CONCLUSIONS

We have introduced a new receiver architecture based on the combination of MIMO processing and MLSE detection. The primary application of this receiver is electronic dispersion compensation in MMF optical communications, although many other applications are possible. This receiver is able to compensate for both the impairments of the MMF and those arising from imperfections of the interleaved analog front end. Using an IEEE 802.3aq fiber database, we have shown that this receiver performs at least 2dB better than a traditional DFE on 99% of the LAN fiber population. If limitations of analog DFE implementations proposed in recent literature are taken into account, the benefit of the architecture introduced here increases to at least 4dB. The receiver lends itself well to a single chip implementation in standard 90nm CMOS technology.

ACKNOWLEDGMENTS

The authors wish to thank Dr. Paul Voois for developing OCCAM and making it available for this work.

REFERENCES

- [1] *IEEE 802.3aq Task Force*. [Online]. Available: <http://www.ieee802.org/3/aa/>
- [2] "Gen 67 FDDI Monte Carlo data set," *IEEE 802.3aq Task Force*, Jan. 2005. [Online]. Available: <http://grouper.ieee.org/groups/802/3/aa/public/tools/MonteDCarlo/OM1>
- [3] A. Petraglia and S. K. Mitra, "Analysis of mismatch effects among A/D converters in a time-interleaved waveform digitizer," *IEEE Trans. Instrum. Meas.*, vol. 40, no. 5, pp. 831–835, Oct. 1991.
- [4] H. F. Haunstein *et al.*, "Principles for electronic equalization for polarization-mode dispersion," *IEEE J. Lightwave Technol.*, vol. 22, no. 4, pp. 1169–1182, Apr. 2004.
- [5] A. J. Weiss, "On the performance of electrical equalization in optical fiber transmission systems," *IEEE Photon. Technol. Lett.*, vol. 15, no. 9, pp. 1225–1227, Sept. 2003.
- [6] O. E. Agazzi, M. R. Hueda, H. S. Carrer, and D. E. Crivelli, "Maximum likelihood sequence estimation in dispersive optical channels," *IEEE J. Lightwave Technol.*, vol. 23, no. 2, pp. 749–763, Feb. 2005.
- [7] B. L. Kasper, "Equalization of multimode optical fiber systems," *Bell Syst. Tech. Journal*, vol. 61, no. 7, p. 1367, Sept. 1982.
- [8] C. Xia, M. Ajgaonkar, and W. Rosenkranz, "On the performance of the electrical equalization technique in MMF+ links for 10 gigabit ethernet," *IEEE J. Lightwave Technol.*, vol. 23, no. 6, pp. 2001–2011, June 2005.
- [9] W. Rosenkranz and C. Xia, "Advanced electronic equalization for high-speed data transmission over multi-mode as well as single-mode optical fiber," in *Proc. of the European Conference on Optical Communications (ECOC)*, 2005.
- [10] T. Nielsen and S. Chandrasekar, "OFC 2004 workshop on optical and electronic mitigation of impairments," *IEEE J. Lightwave Technol.*, vol. 23, no. 1, pp. 131–142, Jan. 2005.
- [11] "108 fiber model," *IEEE 802.3aq Task Force*, Oct. 2004. [Online]. Available: <http://grouper.ieee.org/groups/802/3/aa/public/tools/108fiberModel>
- [12] W. C. Black and D. A. Hodges, "Time-interleaved converter arrays," *IEEE J. Solid-State Circuits*, vol. 15, no. 6, pp. 1022–1029, Dec. 1980.
- [13] M. Webster *et al.*, "A statistical analysis of conditioned launch for gigabit ethernet links using multimode fiber," *IEEE J. Lightwave Technol.*, vol. 17, no. 9, pp. 1532–1541, Sept. 1999.
- [14] J. King, "Experiments on time variation due to polarization and mmf shaking and results," *IEEE 802.3aq Task Force*, Nov. 2004. [Online]. Available: http://www.ieee802.org/3/aa/nov04/king_2_1104.pdf
- [15] J. Shaw, D. Cunningham, and S. Meadowcroft, "Variation of pie-d in multimode fibre due to polarization, mechanical stress, and connector offset," *IEEE 802.3aq Task Force*, Jan. 2005. [Online]. Available: http://www.ieee802.org/3/aa/public/jan05/meadowcroft_1_0105.pdf
- [16] G. P. Agrawal, *Fiber-Optic Communication Systems*. Wiley-Interscience, 1997.
- [17] J. R. Barry, E. A. Lee, and D. G. Messerschmitt, *Digital Communication*, 3rd ed. KAP, 2004.
- [18] G. D. Forney, "Maximum-likelihood sequence estimation of digital sequences in the presence of intersymbol interference," *IEEE Trans. Commun.*, vol. 18, no. 3, pp. 363–378, May 1972.
- [19] P. J. Black and T. H. Y. Meng, "A 1Gb/s, four-state, sliding block Viterbi decoder," *IEEE J. Solid-State Circuits*, vol. 32, no. 6, pp. 797–805, June 1997.
- [20] K. K. Parhi, *VLSI Signal Processing Systems: Design and Implementation*. Wiley Inter-Science, 1999.
- [21] MATLAB, "Software package version 6.1," *The MathWorks, Inc.*, June 2002.
- [22] S. Bhoja, "Channel metrics for edc-based 10gbase-lrm," *IEEE 802.3aq Task Force*, July 2004. [Online]. Available: http://grouper.ieee.org/groups/802/3/aa/public/jul04/bhoja_1_0704.pdf
- [23] A. Reynolds *et al.*, "A 7-tap transverse analog-FIR filter in 0.13μm CMOS for equalization of 10Gb/s fiber-optic data systems," *International Solid-State Circuits Conference (ISSCC)*, pp. 330–331, Feb. 2005.
- [24] N. Swenson *et al.*, "Explanation of IEEE 802.3, clause 68 TWDP." [Online]. Available: <http://ieee802.org/3/aa/public/tools/TWDP.pdf>
- [25] B. Razavi, *Principles of Data Conversion System Design*. Wiley Interscience, 1995.
- [26] N. Kurosawa *et al.*, "Explicit analysis of channel mismatch effects in time-interleaved ADC systems," *IEEE Trans. Circuits Syst. I*, vol. 48, no. 3, pp. 261–271, Mar. 2001.